

## Prospects for Higgs boson searches at the Large Hadron Collider

B MELLADO

Physics Department, University of Wisconsin-Madison, Madison, Wisconsin 53706, USA  
E-mail: bmellado@mail.cern.ch

**Abstract.** These proceedings summarize the sensitivity for the CMS and ATLAS experiments at the LHC to discover a Standard Model Higgs boson with relatively low integrated luminosity per experiment. The most relevant discovery modes are dealt with. A brief discussion on the expected performance from these experiments in searches for one or more of the Higgs bosons from the minimal version of the supersymmetric theories is also included.

**Keywords.** Large hadron collider; Higgs boson; Standard Model.

**PACS Nos** 12.15.-y; 13.85.-t; 14.80.Bn; 14.80.Cp

### 1. Introduction

In the Standard Model (SM) of electroweak and strong interactions, there are four types of gauge vector bosons (gluon, photon,  $W$  and  $Z$ ). The SM also predicts the existence of one scalar boson, the Higgs boson [1,2]. The observation of the Higgs boson remains one of the major cornerstones of the SM. This is the primary focus of the CMS and ATLAS Collaborations at the Large Hadron Collider.

The Higgs mass is not predicted by theory and, to date, direct experimental searches for the Higgs have put a lower limit on its mass at  $M_H > 114.4 \text{ GeV}/c^2$  at 95% confidence level (CL) [3]. The preferred value for the Higgs mass, derived by fitting precision electroweak data [4] is currently  $M_H = 87^{+36}_{-27} \text{ GeV}/c^2$  with an upper bound of  $160 \text{ GeV}/c^2$  at 95% CL.

Both the CMS and ATLAS experiments at the LHC, scheduled for proton–proton collision data-taking from 2008, have been designed to search for the Higgs over a wide mass range [5,6]. These proceedings summarize the sensitivity for each experiment to discover a SM Higgs boson with relatively low integrated luminosity per experiment ( $1\text{--}30 \text{ fb}^{-1}$ ) as well as recent developments that have enhanced this sensitivity.

The Standard Model Higgs boson will be produced at the LHC via several mechanisms. The Higgs boson will be predominantly produced via gluon–gluon fusion [7] (see the left diagram in figure 1). For Higgs boson masses, such that  $M_H > 100$

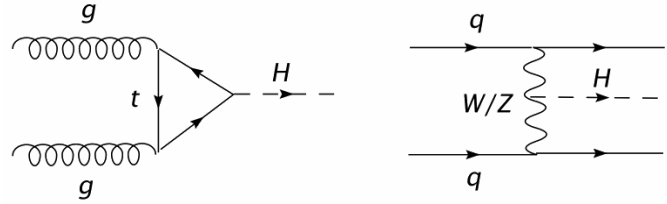


**Figure 1.** Leading order diagrams for the dominant processes involving the production of a SM Higgs boson at the LHC: gluon–gluon fusion (left) and vector boson fusion (right).

$\text{GeV}/c^2$ , the second dominant process is the vector boson fusion (VBF) [8,9] (see right diagram in figure 1).

In addition to inclusive searches, the CMS and ATLAS Collaborations have investigated the feasibility of observing the Higgs in association with at least one or two high transverse momentum,  $p_T$ , hadronic jets. In the case of gluon–gluon fusion the Higgs can be produced alone. However, when one of the gluons or top quarks emits a gluon, the Higgs is produced with the gluon, which is seen in the detector as a hadronic jet. In the case of vector boson fusion, the Higgs is produced with at least two jets. In both cases, jets produced in association with the Higgs are most useful for the identification of the Higgs boson, suppressing significantly the QCD backgrounds.

Efforts have been developed to understand the sensitivity of the detectors for the minimal expression of the Higgs sector, a single Higgs doublet. With the extension of the Higgs sector by the addition of a second Higgs doublet, the situation becomes more complex, as the multiplicity of relevant final states is enhanced. In the latter case, the Higgs sector contains two charged ( $H^\pm$ ) and three neutral ( $h, H, A$ ) physical states. All Higgs boson masses and couplings are expressed in terms of two parameters: the mass of the CP-odd boson,  $m_A$ , and the ratio of the vacuum expectation values of the Higgs doublets,  $\tan\beta$ .

A brief discussion on the sensitivity for these experiments to discover one or more of the Higgs bosons from the minimal version of the supersymmetric theories [10] (MSSM) is also included. Here we consider the case where the mass of supersymmetric particles are large enough so that they do not play an important role in the phenomenology.

## 2. Standard Model Higgs production at the LHC

The SM Higgs production cross-sections at the LHC to QCD next-to-leading-order (NLO), as a function of Higgs mass, are shown in figure 2 (cross-sections were computed with [11]). The dominant production mechanism for SM Higgs boson production, which proceeds via a top-quark loop, is the gluon–gluon fusion mode. The Higgs boson cross-section with this mechanism reaches over 30 pb for masses around  $100 \text{ GeV}/c^2$ . The vector boson fusion process is the second most dominant production mode at the LHC. It typically takes up  $\approx 10\%$  of the total Higgs cross-section for low masses and up to  $\approx 50\%$  for a very heavy Higgs boson. Associated

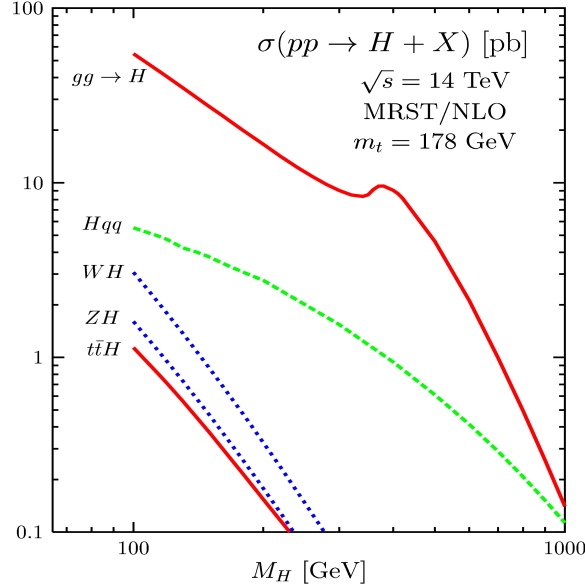


**Figure 2.** Dominant Standard Model Higgs production cross-sections at the LHC. Cross-sections were computed to QCD next-to-leading-order.

production modes, where the Higgs is produced via  $q\bar{q}' \rightarrow HW$ ,  $q\bar{q} \rightarrow HZ$  and  $gg, q\bar{q} \rightarrow t\bar{t}H$ , have smaller cross-sections. The presence of a  $W$ ,  $Z$  or top-quark alongside the Higgs, or high- $p_T$  high- $\eta$  jets from VBF, allow for triggering on events with Higgs in invisible final states.

### 3. Discovery modes for the SM Higgs boson

The final states most suitable for discovery at the LHC vary depending on the branching ratios, shown in figure 3 (branching ratios were computed with [11]), which are a function of the Higgs mass, and the relevant backgrounds. For  $M_H < 2M_W$  the dominant decay mode is through  $b\bar{b}$ . However, due to the enormous QCD background, this channel is only considered in the  $t\bar{t}H$  final state where handles exist for the rejection of this background [11a]. The  $\gamma\gamma$  final state, which appears when the Higgs decays via bottom, top and  $W$  loops, has a small branching fraction but excellent  $\gamma$ /jet separation and  $\gamma$  resolution help to make this a very significant channel. The  $H \rightarrow \tau^+\tau^-$  decay is accessible through the VBF modes, where the two struck quarks appear as high- $p_T$  jets in the very forward (high- $\eta$ ) and opposite regions of the detectors (backward-forward).

If the Higgs mass is large enough to make the  $WW$  and  $ZZ$  modes kinematically accessible, the  $H \rightarrow WW^{(*)}$  final states are powerful over a very large mass range ( $WW$  accounts for  $\sim 95\%$  of the branching ratio at  $M_H \sim 160 \text{ GeV}/c^2$ ), as is the  $H \rightarrow ZZ^{(*)} \rightarrow 4l$  final state – the latter is commonly referred to as the ‘golden

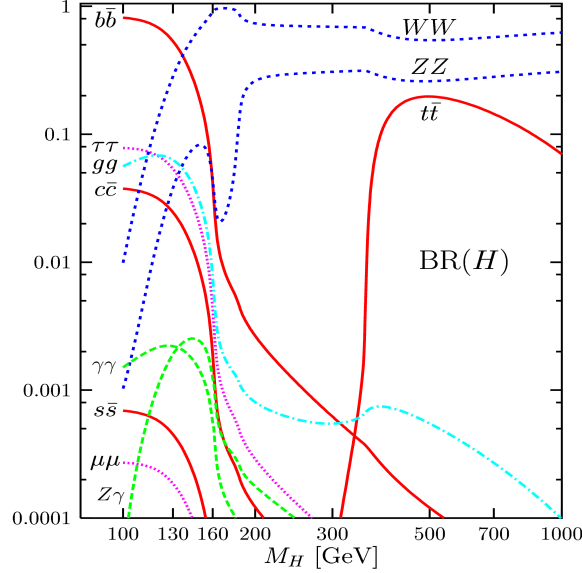


**Figure 3.** Branching ratios for standard model Higgs decays.

mode’ as with four leptons in the final state the signal is easy to trigger on and allows for full reconstruction of the Higgs mass.

Both CMS and ATLAS have conducted extensive fully simulated GEANT-based [12] Monte Carlo studies to determine the experimental viability of all these channels. A few of these signatures are highlighted below. A more comprehensive and complete account can be found elsewhere [5,6,13,14].

### 3.1 $H \rightarrow \gamma\gamma$

Despite the small branching ratio,  $H \rightarrow \gamma\gamma$  remains a very attractive channel for  $M_H < 140 \text{ GeV}/c^2$ . The backgrounds to this channel are usually divided into two types: irreducible and reducible. Photon pairs from  $q\bar{q} \rightarrow \gamma\gamma$ ,  $gg \rightarrow \gamma\gamma$  and quasi-collinear quark bremsstrahlung comprise the irreducible background, while jet-jet and  $\gamma$ -jet events, where one or more jets are misidentified as photons (mostly from the production of energetic  $\pi^0$ s), take up the bulk of the reducible background.  $Z \rightarrow e^+e^-$  events, with both electrons misidentified as photons, can be reduced using electron/photon separation techniques. The high-granularity liquid argon calorimeter of ATLAS is capable to resolve single photons from  $\pi^0$ s, while CMS has a superior energy resolution [14a]. Studies of the inclusive analysis conducted by both experiments consider the signal and backgrounds to QCD NLO. Both experiments have looked beyond a simple cut-based analysis. The discriminating power of the di-photon transverse momentum and the photon decay angle in the Higgs boson rest frame with respect to the Higgs boson lab flight direction,  $|\cos \theta^*|$ , are evaluated in conjunction with the di-photon invariant mass.

## Prospects for Higgs boson searches at the LHC

Efforts have been made to evaluate the feasibility of Higgs boson searches in association with at least one or two high  $p_T$  hadronic jets. The sensitivity of the Higgs boson production in association with  $Z, W$  and  $t\bar{t}$  has also been evaluated. Their relevance to the measurement of Higgs couplings has been evaluated.

The sensitivity of this channel is similar for both experiments. For  $M_H = 130$  GeV/ $c^2$ , and an integrated luminosity of  $30 \text{ fb}^{-1}$  more than a  $5\sigma$  effect may be achieved.

### 3.2 $H \rightarrow \tau^+\tau^-$

The distinct experimental signature of Higgs production via VBF, with jets from the ‘struck quarks’ at high- $\eta$  and Higgs decay products in the central region is a great asset for channels like  $H \rightarrow \tau^+\tau^-$ . CMS and ATLAS now both consider three final states, thus covering all combinations of leptonically- and hadronically-decaying taus. Triggering on the fully hadronic mode by using combinations of low- $p_T$  tau and other triggers (e.g., missing transverse energy or forward jets) are currently under investigation. Despite the presence of multiple neutrinos in the final state, mass reconstruction can typically be done via the collinear approximation where the tau decay daughters are assumed to be in the same direction as their parent. The resolution on the reconstructed mass ( $\sim 10$  GeV/ $c^2$  for  $M_H = 120$  GeV/ $c^2$ ) is mainly affected by the missing energy resolution. Data-driven methods for understanding the dominant backgrounds ( $Z$  + jets, QCD and  $t\bar{t}$ ) have been investigated.

### 3.3 $H \rightarrow ZZ^{(*)} \rightarrow 4l$ ( $4e, 4\mu, 2e2\mu$ )

At  $M_H > 130$  GeV/ $c^2$ , the 4-lepton channels gain in importance on account of the precise energy reconstruction of both ATLAS and CMS for electrons and muons. The dominant backgrounds for these channels are  $ZZ^{(*)}$ ,  $Zb\bar{b}$  and  $t\bar{t}$  production. Through the use of impact parameter and lepton isolation requirements the latter two can be significantly reduced. The  $q\bar{q}$  component of the  $ZZ^{(*)}$  background is known at NLO, however due to the lack of a Monte Carlo generator for  $gg \rightarrow ZZ^{(*)}$ , typically the contribution from this process is added as 30% of the LO  $q\bar{q} \rightarrow ZZ^{(*)}$  [15a]. After the imposition of an appropriate event selection the contribution of the reducible  $Zb\bar{b}$  and  $t\bar{t}$  backgrounds becomes negligible for searches of a heavy Higgs boson and becomes significantly smaller than the contribution of reducible backgrounds for low mass Higgs boson searches. Collectively, the significance for these channels is more than  $5\sigma$  for  $30 \text{ fb}^{-1}$  of data.

### 3.4 $H \rightarrow WW^{(*)} \rightarrow l\nu l\nu$ ( $l = e, \mu$ )

As the branching ratio for a SM Higgs decaying to  $WW$  is more than 95% at  $\sim 160$  GeV/ $c^2$ , this is the most significant channel at that mass point. Unlike other channels, in the  $H \rightarrow WW \rightarrow l\nu l\nu$  final state full mass reconstruction is not possible and the analysis is essentially reduced to a counting experiment; therefore

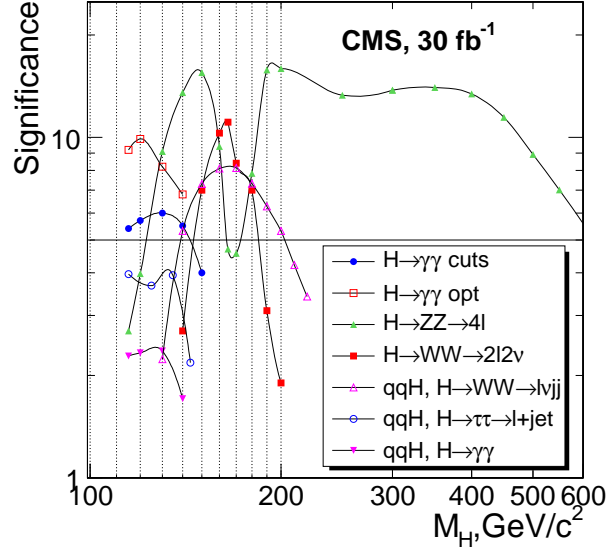


**Figure 4.** The discovery potential at CMS for Standard Model Higgs boson searches, as obtained using NLO cross-sections, for  $30 \text{ fb}^{-1}$ .

an accurate background estimate is critical. The dominant backgrounds for this analysis are  $W^+W^-$  and  $t\bar{t}$  production. The former can be suppressed by exploiting spin correlations between the two leptons while the latter has been shown to be suppressed significantly by a jet veto. The analysis is performed in two regimes: with the application of a full jet veto [15b] and with the tagging of two high  $p_T$  hadronic jets [15c].

Using NLO cross-sections and conservative estimates for the effect of systematic uncertainties, a significance of around  $5\sigma$  for  $M_H = 165 \text{ GeV}/c^2$  using an integrated luminosity of  $\sim 1 \text{ fb}^{-1}$  is estimated. The sensitivity of this channel is also evaluated for other Higgs boson masses showing strong sensitivity for the mass range  $140 < M_H < 190 \text{ GeV}/c^2$ .

#### 4. Summary of Higgs discovery potential

The expected significance in  $30 \text{ fb}^{-1}$ , for various final states as a function of SM Higgs mass, is summarized in figure 4 for the CMS experiment. The discovery potential at CMS and ATLAS is quite similar.

Discovery prospects for the detection of MSSM Higgses ( $A$ ,  $h$ ,  $H$  and  $H^\pm$ ) have also been evaluated [5,6]. At tree-level, all Higgs masses and couplings can be expressed in terms of  $m_A$  and  $\tan\beta$ . The complete region of the  $m_A - \tan\beta$  parameter space ( $m_A = 50\text{--}500 \text{ GeV}/c^2$  and  $\tan\beta = 1\text{--}50$ ) should be accessible to the LHC experiments. The sensitivity for the discovery of MSSM Higgses, in the minimal mixing scenario for  $30 \text{ fb}^{-1}$  of data, is summarized in figure 5 for the ATLAS experiment. As in the case of the SM Higgs boson, the discovery potential at CMS and ATLAS is quite similar.

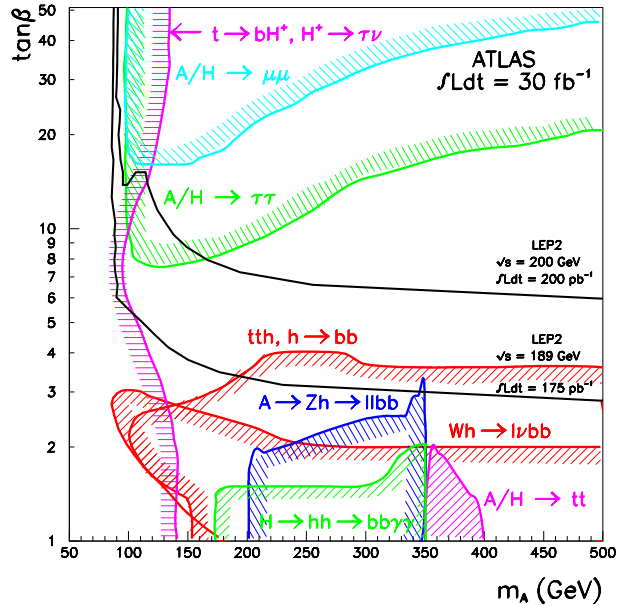


**Figure 5.** ATLAS sensitivity for the discovery of MSSM Higgs bosons (minimal mixing scenario). The  $5\sigma$  discovery contour curves are shown in the  $m_A$ - $\tan\beta$  plane for  $30\text{ fb}^{-1}$ . Performance with CMS is similar.

### Acknowledgments

I would like to thank Dr T Vickey for his extensive help with the text.

### References

- [1] F Englert and R Brout, *Phys. Rev. Lett.* **13**, 321 (1964)  
P W Higgs, *Phys. Lett.* **B12**, 132 (1964)  
P W Higgs, *Phys. Rev. Lett.* **13**, 508 (1964)
- [2] A Djouadi, hep-ph/0503172 and references therein
- [3] LEP Higgs Working Group: *Phys. Lett.* **B565**, 61 (2003)
- [4] The LEP Electroweak Working Group, <http://lepewwg.web.cern.ch/>
- [5] CMS Physics TDR, CERN-LHCC 2006-021
- [6] ATLAS Physics TDR, CERN-LHCC 99-14/15
- [7] H M Georgi, S L Glashow, M E Machacek and D V Nanopoulos, *Phys. Rev. Lett.* **40**, 692 (1978)
- [8] R Cahn and S Dawson, *Phys. Lett.* **B136**, 196 (1984)
- [9] G Kane, W Repko and W Rolnick, *Phys. Lett.* **B148**, 367 (1984)
- [10] J Wess and B Zumino, *Nucl. Phys.* **B70**, 39 (1974); *idem*, *Phys. Lett.* **B49**, 52 (1974)  
P Fayet, *Phys. Lett.* **B69**, 489 (1977); *ibid.* **84**, 421 (1979); *ibid.* **86**, 272 (1979)
- [11] M Spira, <http://people.web.psi.ch/spira/>
- [11a] The observation of a Higgs boson with the  $b\bar{b}$  decay in association with  $t\bar{t}$  is not considered here as a discovery channel

*B Mellado*

- [12] S Agostinelli *et al*, *Nucl. Instrum. Methods* **A506**, 250 (2003)  
J Allison *et al*, *IEEE Trans. Nucl. Sci.* **53(1)**, 270 (2006)
- [13] ATLAS Collaboration: S Asai *et al*, *Eur. Phys. J.* **C32**, 19 (2004)
- [14] ATLAS CSC notes, to be submitted
- [14a] Detailed comparisons of the sensitivity of the two experiments are underway
- [15] T Binoth, N Kauer and P Mertsch, Gluon-induced QCD corrections to  $pp \rightarrow ZZ \rightarrow \bar{l}l'\bar{l}'$ , To appear in the *Proceedings of 16th International Workshop on Deep Inelastic Scattering and Related Subjects (DIS 2008)* (London, England, 7–11 Apr. 2008), e-Print: arXiv:0807.0024 [hep-ph]
- [15a] Currently, the `gg2ZZ` generator is being used in order to properly take into account the  $gg \rightarrow ZZ^{(*)}$  process, including  $Z/\gamma$  interference effects [15]
- [15b] Events are rejected in which a hadronic jet is found with  $p_T > 20$  GeV/c (hadron level) in the pseudorapidity range  $|\eta| < 4.9$ . With this selection the leading background is the non-resonant production of  $W^+W^-$
- [15c] This analysis is designed to isolate the VBF signal. The leading background is the  $t\bar{t}$  production